Accurate reconstruction of the *jV*-characteristic of organic solar cells from measurements of the external quantum efficiency

Toni Meyer,[a] Christian Körner, Koen Vandewal, and Karl Leo[b]
Dresden Integrated Center for Applied Physics and Photonic Materials, Technische Universität Dresden, Nöthnitzer Str. 61, 01062 Dresden, Germany

(Received 13 October 2017; accepted 20 March 2018; published online 2 April 2018)

In two terminal tandem solar cells, the current density - voltage (*jV*) characteristic of the individual subcells is typically not directly measurable, but often required for a rigorous device characterization. In this work, we reconstruct the *jV*-characteristic of organic solar cells from measurements of the external quantum efficiency under applied bias voltages and illumination. We show that it is necessary to perform a bias irradiance variation at each voltage and subsequently conduct a mathematical correction of the differential to the absolute external quantum efficiency to obtain an accurate *jV*-characteristic. Furthermore, we show that measuring the external quantum efficiency as a function of voltage for a single bias irradiance of 0.36 AM1.5g equivalent sun provides a good approximation of the photocurrent density over voltage curve. The method is tested on a selection of efficient, common single-junctions. The obtained conclusions can easily be transferred to multi-junction devices with serially connected subcells. *Published by AIP Publishing.* https://doi.org/10.1063/1.5009155

I. INTRODUCTION

Even though the first organic photovoltaic bilayer device showing the photoelectric effect was introduced in 1958,[1] it took nearly three more decades until the importance of the topic was essentially recognized in 1986 through the work of Tang,[2] who showed an organic photovoltaic bilayer device with a power conversion efficiency (PCE) of almost 1%. Due to its attractive features such as low cost, flexibility, and low weight, research on organic photovoltaic devices attracted an increasing attention over the years. This led to a gradual increase in the device efficiency with an up-to-date efficiency of 14.1% for a fully solution processed ternary polymer:non-fullerene:fullerene single cell.[3] Besides the synthesis of novel materials with improved characteristics, a proven way to further increase the device performance is to fabricate multi-junction devices, where two or more single-junctions are stacked on top of each other. The most common representative of this device class is the serial double-junction or the serial tandem solar cell (sTSC). Its main advantage is the possibility of combining solar cells with, in the best case, fully complementary absorption. This typically involves the usage of absorber materials with different optical gaps, which additionally reduces the losses due to thermalization of excess energy of the excited charges. The best organic sTSC recently being published reached a PCE of 13.8%.[4]

One challenge regarding the characterization of sTSC is resolving the *jV*-characteristics of the individual single-junctions, the so called subcells of the multi-junction. Due to the lack of a third terminal, a direct measurement of the subcells' *jV*-characteristics is not possible. However, the spectra of the external quantum efficiency (*EQE*) of the subcells can be resolved by selecting appropriate bias illumination.[5] Gilot *et al.*[6] introduced a method utilizing such *EQE*-measurements to indirectly reconstruct the *jV*-characteristics of the subcells, which was used in a simplified form by Timmreck *et al.*[7] A series of *EQE*-measurements with a variable additional external bias voltage is conducted at the subcells. From these *EQE*-measurements, the integrated photocurrent for each single *EQE*-measurement can be calculated with respect to the standard AM1.5g spectrum. Next, the dark-characteristic of the sTSC is added to the photocurrent. As a last step, a rectification with the open-circuit voltage of the non-limiting subcell, as assumed from the single cell, is done to obtain the *jV*-characteristic of the subcell. Hence, this method, hereafter called the *EQEjV*-method, enables the indirect measurement of the total *jV*-characteristic of each subcell without the introduction of an additional terminal. Additionally, the *jV*-characteristic of the total sTSC can be determined.

In this work, we show that further precautions have to be taken to obtain results with improved accuracy with the *EQEjV*-method. Organic solar cells often inhibit a sublinear behavior of the photocurrent with respect to the irradiance. In this case, the *EQE* and its equivalent, the spectral response (*SR*), depend on the irradiance. Additionally, the measurement of the *EQE* is a measurement of a differential quantity due to it being commonly conducted with chopped monochromatic illumination, i.e., the differential *EQE* (*dEQE*) or differential spectral response (*DSR*) is measured. To obtain the correct absolute height of the *EQE* for a certain illumination condition of the solar cell, a mathematical correction of the *DSR* to the absolute *SR* has to be performed as proposed by Metzdorf.[8] A requirement for this correction, is the measurement of the *DSR* at multiple bias irradiance conditions. Thus, for sTSC, it commonly is not sufficient to flood only the non-limiting subcell with charge carriers. Even though,

[a]toni.meyer@iapp.de
[b]karl.leo@iapp.de

this leads to the distinct limitation of the subcell, it typically is measured at only one arbitrary irradiance.[7] In the original introduction of the method, measuring the *dEQE* without any bias illumination, again for AM1.5g equivalent illumination and performing a correction with the relation between both measurements for all subsequent measurements leads to a sufficient accuracy, at least for good solar cells.[6] However, we show that for an improved accuracy, the *dEQE* has to be measured at multiple bias irradiances at all voltage points to perform the mathematical correction to the absolute quantity for each voltage point individually. This is necessary, because the *EQE* often decreases for elevated intensities due to bimolecular recombination of which the rate depends on the charge carrier density in the device. Furthermore, this decrease is unique at every voltage point due to an altered extraction of the charge carriers.[9] In this work, we show the impact of the bias irradiance on the integrated differential photocurrent density of the *dEQE*-measurement. We perform the construction of the *EQEjV* in different ways and show the consequences for the accuracy of the *EQEjV*-method for a selection of efficient, common small molecule single-junctions. Even though we investigate only single-junctions, the results can easily be transferred to the measurement of subcells of multi-junction devices. The selection consists of a cascade,[10] three planar-mixed heterojunctions, denoted by their bulk-heterojunction (BHJ) donor materials DCV5T-Me,[11] F_4-ZnPc,[12] and BDP-OMe,[13] and a planar-mixed-planar heterojunction likewise denoted by its BHJ donor material Ph_2-benz-BODIPY.[14,15] The presented results show in all cases that it is necessary to perform the whole measurement procedure at all voltages to obtain the correct short-circuit current density (j_{sc}) and fill factor (*FF*) from the reconstruction of the *jV*-characteristic. Furthermore, based on the results, we suggest that for a good approximation of the reconstructed *jV*-characteristic, a voltage dependent measurement series of the *dEQE* for only one bias irradiance of 0.36 AM1.5g sun equivalents can be conducted.

II. EXPERIMENTAL

A. Fabrication

All layers of the presented devices were fabricated by thermal evaporation in a high vacuum chamber (K. J. Lesker, UK) with a base pressure of around 10^{-8} mbar. Glass (TFD, USA) with prestructured indium tin oxide (ITO, 90 nm with 26 Ω/sq and 84% transparency) electrodes served as a substrate. In the cascade, α–6T was used as the donor and deposited at a rate of 1 Å/s. SubPc and SubNc served as acceptors and both were deposited at a rate of 0.5 Å/s. The BHJs were fabricated by simultaneous coevaporation of the donor and acceptor material from different crucibles. C_{60} was used as the acceptor in all BHJs. The DCV5T-Me BHJ was deposited with a substrate temperature of 90 °C, a rate of 0.2 Å/s, and a volume ratio of 2:1. The F_4-ZnPc BHJ was deposited with a substrate temperature of 95 °C, a rate of 0.3 Å/s, and a volume ratio of 1:1. The BDP-OMe BHJ was deposited with a substrate temperature of 100 °C, a rate of 0.3 Å/s, and a volume ratio of 1:2. The Ph_2-benz-BODIPY BHJ was deposited with a substrate temperature of 95 °C, a rate of 0.4 Å/s, and a volume ratio of 1:3. Additionally, neat SubNc deposited at a rate of 0.3 Å/s was used as an additional absorber on the hole side of the Ph_2-benz-BODIPY device. In the BHJ devices, neat C_{60} or neat C_{70} both being deposited at a rate of 0.4 Å/s, were used on the electron side as exciton reflecting and hole blocking layer furthermore serving as an active layer with a small contribution to the current. In the BHJ devices, either intrinsic 9,9-bis[4–(N,N-bis-biphenyl-4-yl-amino)phenyl]-9H-fluorene (BPAPF) or intrinsic N,N′-((Diphenyl-N,N′-bis)9,9,-dimethyl-fluoren-2-yl)-benzidine (BF-DPB) served as the exciton reflecting and electron blocking layer on the hole side. For the BDP-OMe device and the Ph_2-benz-BODIPY device, the matrix material of the electron transport layer (ETL) was N,N-Bis(fluoren-2-yl)-naphthalenetetracarboxylic diimide (Bis-Hfl-NTCDI). For the F_4-ZnPc device, C_{60} served as the matrix material for the ETL. In case of the F_4-ZnPc, the BDP-OMe, and the Ph_2-benz-BODIPY devices, the ETL-matrix always was doped with 7 wt. % of tetrakis(1,3,4,6,7,8-hexahydro-2H-pyrimido[1,2-a]pyrimidinato)-ditungsten (II) [W_2(hpp)$_4$], except for the F_4-ZnPc device were 3 wt. % were used. For the DCV5T-Me device, a mixed layer of 4,7-diphenyl-1,10-phenanthroline (BPhen) and Cs with a volume ration of 1:1 was used as the ETL. For the cascade, neat BPhen was used as the ETL. In case of the BHJ devices, either BPAPF or BF-DPB served as the matrix for the hole transport layer (HTL). For all BHJ devices, the HTL-matrix was doped with 10 wt. % NDP9 (Novaled AG). For all BHJ devices, a 1 nm layer of pure NDP9 was used to assure ohmic contact. For all BHJ devices, 100 nm Al served as the top electrode. For the cascade, 100 nm Ag served as the top electrode. The following densities (ρ) were used for the mass and accordingly thickness determination by quartz crystal microbalance: $\rho(C_{60}) = 1.63\ g/cm^3$, $\rho(C_{70}) = 1.56\ g/cm^3$, ρ(DCV5T-Me) $= 1.30\ g/cm^3$, ρ(α–6T) $= 1.40\ g/cm^3$, ρ(SubPc) $= 1.50\ g/cm^3$, ρ(SubNc) $= 1.50\ g/cm^3$, $\rho(Ph_2$-benz-BODIPY) $= 1.09\ g/cm^3$, $\rho(F_4$-ZnPc) $= 1.30\ g/cm^3$, ρ(Bis-Hfl-NTCDI) $= 1.25\ g/cm^3$, ρ(BPAPF) $= 1.20\ g/cm^3$, ρ(BF-DPB) $= 1.21\ g/cm^3$, ρ(BPhen) $= 1.24\ g/cm^3$, ρ(Ag) $= 10.50\ g/cm^3$, and ρ(Al) $= 2.73\ g/cm^3$. For the doped layers, the density of the dopants was set to the density of the matrix material. The cross section between the ITO bottom electrode and the metal top electrode defines the size of the unmasked active area of 6.44 mm^2 for all presented samples. The complete stack of the devices can be found in the supplementary material.

B. Characterization

The *EQE*-spectra were measured using a lock-in amplifier (Signal Recovery SR 7265, Ametek Scientific Instruments, USA) detecting the frequency modulated current response generated by the monochromatic, chopped illumination irradiance (Oriel Xenon Arc-Lamp Apex Illuminator combined with Cornerstone 260 1/4 m monochromator, Newport, USA). The SR570 low-noise current preamplifier (Stanford Research Systems, USA) was used for signal amplification and applying the bias voltage. For the measurement of the illumination spectrum, a mono-crystalline Si reference diode (S1337–33BQ, Hamamatsu, Japan) was used. A Xenon lamp solar simulator

(16 S-003–300, Solarlight Company, Inc., USA) in combination with a filter wheel utilizing neutral density metal-grid filters for setting the irradiance served as bias light. For the measurement of the *jV*-characteristics, a source measure unit (Keithley SMU2400, USA) was employed. The illumination spectrum provided by a Xenon lamp solar simulator (16 S-003–300, Solarlight Company, Inc., USA) was monitored with a mono-crystalline Si reference diode (S1337–33BQ, Hamamatsu, Japan). The spectra of the light sources were measured with a CAS 140T spectrometer (Instrument Systems, Germany). The solar simulator spectrum was mismatch corrected to provide AM1.5g equivalent illumination for an intensity of 100 mW/cm^2. The total measurement procedure for one sample was performed as follows: first, the *dEQE* of each sample was measured to determine the spectral mismatch factor for the standard *jV*-characterization. Then, the standard mismatch corrected *jV*-characterization was performed without an aperture mask (6.44 mm^2) and with an aperture mask (3.06–3.09 mm^2). Next, the Python automated measurement series with varying applied bias voltage and varying applied bias irradiance of the Xenon lamp was performed. The different bias irradiances were set with a filter wheel utilizing different neutral density metal-grid filters. The automated measurement series consisted of a stability measurement of the *dEQE* without bias voltage and bias illumination at the beginning, followed by the measurement of the photocurrent generated by the bias irradiance in the test sample for all filter wheels. Afterwards, the voltage series of the *dEQE* was measured for each bias irradiance subsequently going from low to high irradiances. At the beginning of each voltage series, the photocurrent generated by the bias light in the test sample was measured again. The measurement of the photocurrent generated in the test sample by all different bias irradiances was repeated at the end followed by another stability measurement of the *dEQE* without bias voltage and bias illumination. This last stability measurement of the automated measurement series was used to determine the spectral mismatch factor again and repeating the standard *jV*-measurement without and with an aperture mask.

III. RESULTS

A. *EQE* with applied bias voltage and bias illumination

The two quantities dark current and photocurrent are commonly accessible in any lab with a standard solar cell characterization setup. The dark current simply can be measured with a single source measure unit. In contrast, typical *EQE*-setups using the lock-in technique directly separate the photocurrent from the dark characteristic of the device. However, in case of organic solar cells, the photocurrent of the device typically has a sublinear dependence on irradiance, i.e., the *EQE* and its equivalent, the *SR*, likewise depends on the irradiance. Furthermore, a standard measurement of the *EQE* is conducted with chopped monochromatic light. Thus, during the measurement of the *EQE*, the small perturbation due to the chopped monochromatic light on top of a steady-state illumination condition is measured. Hence, the measured *EQE* is a differential quantity instead of an absolute one. Due to the differential measurement, the measured *EQE* will be underestimated if not accounted for as will be shown in the following. This effect was first discussed by McMahon and Sadlon.[16]

In general, the current density can be expressed as

$$j(\lambda, E, V) = SR(\lambda, E, V)E(\lambda), \tag{1}$$

with the wavelength λ, irradiance E, and voltage V. Differentiating Eq. (1) with respect to the irradiance at a constant voltage results in the *DSR*

$$DSR = \frac{dj(\lambda, E)}{dE} = SR(\lambda, E) + E\frac{dSR(\lambda, E)}{dE}. \tag{2}$$

From Eq. (2), it follows that the absolute *SR* is only measured, if the *SR* is not dependent on the irradiance, i.e., $dSR/dE = 0$.[17] Thus, the typical sublinear behavior of the photocurrent of organic solar cells with respect to the irradiance, which implies an irradiance dependent *SR*, leads to the mentioned underestimation of the measured *EQE*. Metzdorf proposed a mathematical correction for transforming the measured *DSR* into the absolute *SR*.[8] This correction algorithm will be used in this work to obtain the correct absolute *EQE* of the solar cells. For a detailed explanation of the correction algorithm, see the publications of Metzdorf or Mundus *et al.*[8,18] To perform the mathematical correction, the *dEQE* has to be measured at multiple bias irradiances as is also required by the standard IEC 60904–8, which defines the requirements for the measurement of linear and nonlinear spectral responsivities. One of these irradiance conditions should exceed the AM1.5g sun equivalent by at least 10%. Furthermore, we show in the following, that this bias irradiance dependent measurement of the *dEQE* has to be performed at all different bias voltages to obtain an accurate absolute photocurrent density over voltage.

In Fig. 1(a), the measurement series of the *dEQE* with varying applied bias voltage and without bias illumination is depicted for the DCV5T-Me solar cell. From this measurement series, the differential photocurrent density over voltage of the device can be derived by calculating the integrated differential photocurrent density with respect to the AM1.5g spectrum for each *dEQE*-measurement at each bias voltage. The result of this calculation for the measurement series without bias illumination (dark) is depicted in Fig. 1(b) for the DCV5T-Me device as a black line. To perform the mathematical correction to the absolute *EQE*, additional measurements with varying applied bias voltage have to be conducted at various bias irradiances. To show the influence of the bias irradiance on the *dEQE*, the construction of the differential photocurrent density over bias voltage was performed for all the measurement series. The results are depicted in Fig. 1(b) and are labeled with *DSR* and its corresponding bias irradiance in AM1.5g equivalent sun. An increasing bias irradiance leads to a steady decrease in the *EQE* caused by a rise of the charge carrier concentration in the device favoring increased bimolecular recombination. Similarly, for an increasing forward bias, the steady-state charge carrier density of photogenerated charges in the device rises due to their decreased extraction. Thus, the *EQE* continuously decreases with increasing forward voltage,

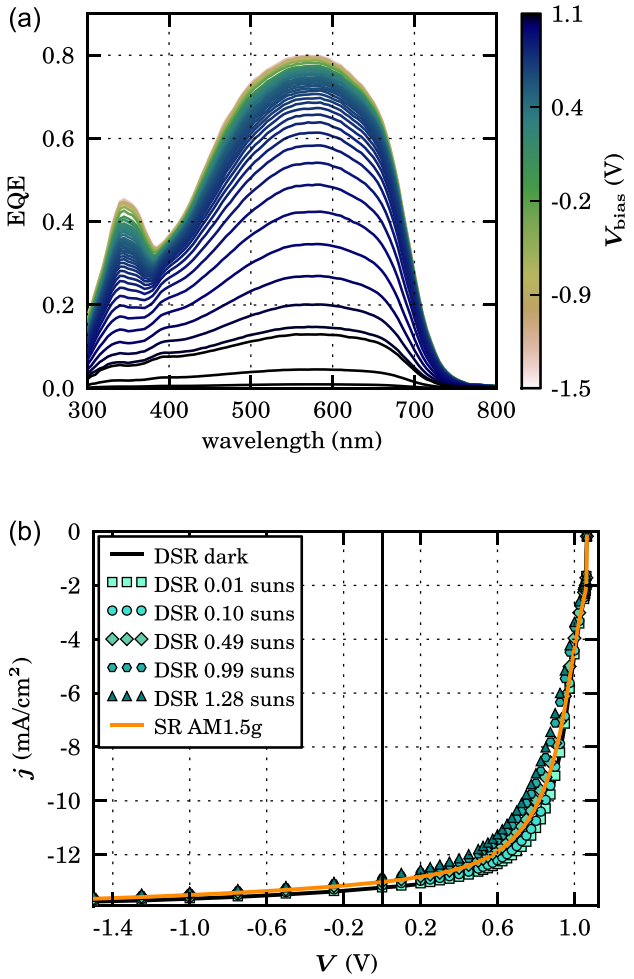

FIG. 1. (a) Differential *EQE*-spectra for the DCV5T-Me device with varying applied bias voltage and without additional bias illumination (dark). (b) Photocurrent density of the DCV5T-Me device derived from the voltage dependent *EQE*-spectra by calculating the integrated photocurrent density with respect to the AM1.5g spectrum. Depicted are the constructions of the differential photocurrent density from the *dEQE* labeled with *DSR* and the bias irradiance in AM1.5g equivalent sun or without bias illumination (dark), as well as the absolute photocurrent density obtained from the mathematical correction performed at each voltage point (*SR* AM1.5g).

because of the decreased extraction accompanied by increased bimolecular recombination.[9] When the forward voltage is sufficiently high, i.e., approximately the built-in voltage of the device, the *EQE* drops to zero. We note that our setup is not sensitive enough to accurately reproduce the expected asymptotic behavior of the photocurrent density for bias voltages above the open circuit voltage of the devices. However, this has no consequences for the presented conclusions. For increasing reverse bias, the *EQE* steadily increases for all investigated samples. Charge carrier extraction[19,20] as well as CT-dissociation[21–24] are promoted until every generated charge is dissociated and extracted.

To obtain the correct absolute height of the *EQE* with respect to the AM1.5g reference spectrum, the mathematical correction of Metzdorf is performed at each voltage individually for the set of bias irradiance dependent measurements of the *dEQE*. The correction yields the set of absolute *EQE*s with respect to the AM1.5g spectrum in dependence of the bias voltage. From this set, the photocurrent density over voltage can be constructed, which is depicted as an orange line (*SR* AM1.5g) in Fig. 1(b). It is clearly visible that the absolute photocurrent density over voltage neither coincides with the differential photocurrent density without bias illumination (*DSR* dark), nor with the differential photocurrent density with AM1.5g equivalent illumination (*DSR* 0.99 sun). The former leads to an overestimation of the photocurrent density, whereas the latter leads to its underestimation. These deviations will transfer to the j_{sc} and *FF* when constructing the *EQEjV* from those measurement series as will be shown in Sec. III B. The dependence of the *dEQE* on bias irradiance varies for the different investigated samples due to a differing magnitude of bimolecular recombination (see supplementary material, Figs. S1b–S5b). The cascade solar cell shows the strongest dependence on bias irradiance, followed by the DCV5T-Me solar cell. The other three investigated solar cells show only a weak dependence on the bias irradiance.

In Fig. 2, the dependence of the integrated differential photocurrent density on bias irradiance at various bias voltages is depicted for the DCV5T-Me solar cell. The measurement series at 0 V is represented by the dash-dotted, green line and the measurement series at the voltage of the maximum power point (V_{mpp}) of 0.75 V is represented by the dashed, dark blue line. The clearly different magnitude of bias irradiance dependence at the various voltages emphasizes the need to examine each voltage point individually. At each voltage point, a bias irradiance dependent measurement of the *dEQE* has to be performed to subsequently conduct the mathematical correction to the absolute *EQE*. Additionally, the absolute integrated photocurrent densities obtained from the mathematical correction are depicted for each voltage as orange markers (*SR* AM1.5g) at the bias irradiance, where measured differential and calculated absolute *EQE* are identical. It is apparent

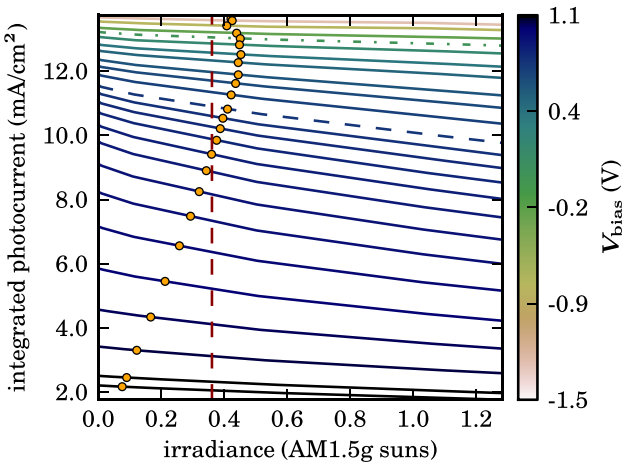

FIG. 2. Dependency of the integrated differential photocurrent density with respect to the AM1.5g spectrum on the bias irradiance for the *dEQE*-measurements for different applied bias voltages for the DCV5T-Me device. The dash-dotted, green line marks 0 V and the dashed, dark blue line marks the voltage of maximum power point of 0.75 V. The orange markers depict the appropriate bias irradiance for approximating the true absolute *EQE* with the *dEQE* for each bias voltage. The vertical, dashed, dark red line marks the bias irradiance leading to the least deviation when approximating the true absolute *EQE* with the *dEQE* over the total voltage range. A reduced dataset regarding the voltage is shown.

that the identity of both quantities shifts to lower bias irradiances for higher forward voltages. Thus, it is not possible to obtain an accurate absolute *EQE* by compensating the effect of the differential measurement through measuring the *dEQE* at one single bias irradiance lower than the AM1.5g equivalent. McMahon *et al*. proposed to use a bias irradiance of 0.37 AM1.5g equivalent sun during the measurement of the *dEQE* for a nonlinearity range α of 0.9–1.1 for minimal deviations when approximating the true absolute *EQE* by the *dEQE*. Furthermore, the standard IEC 60904–8 (Ref. 25) provides fallback provisions for simplified measurement procedures. One simplification suggests to measure the *dEQE* at a bias irradiance of 0.3–0.4 AM1.5g equivalent sun. We derived the ideal bias irradiance for approximating the *EQE* with the *dEQE* for three different cases for all investigated samples (see Table I and corresponding Figs. S19–S21 in the supplementary material). First, the ideal bias irradiance for an approximation at 0 V, where the *EQE* is typically measured, was derived. Second, the ideal bias irradiance for an approximation at the voltage of the maximum power point was derived. Third, the ideal bias irradiance for an approximation over the total voltage range was derived. The latter was determined by minimizing the sum over all voltages of the squared deviation between *dEQE* and *EQE* when varying the bias irradiance. From the average over all samples, we find that for an approximation at 0 V 0.52 AM1.5g equivalent sun is an adequate setting of the bias irradiance for the investigated samples. Additionally, small deviations from this ideal irradiance at 0 V lead only to small errors due to the weak dependency of the integrated differential photocurrent density on bias irradiance. For an approximation at the V_{mpp}, 0.43 AM1.5g equivalent sun is an adequate bias irradiance. The ideal bias irradiance is shifted to lower values due to the stronger dependency of the integrated differential photocurrent density with increasing forward voltage. For the approximation over the total voltage range, we find the average over all samples of 0.36 AM1.5g equivalent sun as the ideal bias irradiance. Due to accounting for even higher voltages than the V_{mpp} with a stronger dependency of the integrated differential photocurrent density on bias irradiance, the ideal bias irradiance shifts to even lower values. The found value of 0.36 AM1.5g equivalent sun for the approximation over the total voltage range fits very well to the value of 0.37 AM1.5g equivalent sun calculated by McMahon *et al*. for minimized errors of this approximation. Furthermore, the ideal bias irradiance for this case fits very well into the bias irradiance range of 0.3–0.4 AM1.5g equivalent sun proposed for the fallback provision of standard IEC 60904–8. Thus, we suggest for evaporated small molecule solar cells to use a bias irradiance of 0.36 AM1.5g equivalent sun when approximating the absolute *EQE* with the *dEQE* for a total voltage series when reconstructing the photocurrent density over the voltage. This approximation should only be used if the total measurement procedure is not feasible or the solar cell is prone to degradation for elevated bias irradiances. The error of this approximation increases with increasing nonlinearities of the devices. The presented data shows, that in the case of sTSC, it does not suffice just to choose a bias irradiance for achieving a distinct limitation by one subcell. For an accurate determination of the photocurrent density over voltage, the total measurement procedure should be conducted as proposed by Metzdorf and the characterization standard IEC 60904–8. If this is not feasible, at least the fallback provision of using a bias irradiance of 0.36 AM1.5g equivalent sun to approximate the absolute *EQE* over the total voltage range should be used. When not following one of the above-mentioned procedures, the photocurrent density over voltage will deviate from the correct value, which leads to inaccuracies of the j_{sc} and the *FF* of the constructed *EQEjV* as will be shown in Sec. III B. Therefore, we strongly suggest to improve the method introduced by Gilot *et al*.[6] by measuring the *dEQE* at various bias irradiances at all voltages and perform the mathematical correction to the absolute *EQE* at each voltage point individually.

TABLE I. Ideal bias irradiance in AM1.5g equivalent sun for approximating the true absolute *EQE* with the measured *dEQE* for three different cases for all investigated samples. The ideal bias irradiances for the approximation at 0 V, at the V_{mpp} and over the total voltage range are shown. The latter was derived by minimizing the sum over all voltages of the squared deviation between *dEQE* and *EQE* when varying the bias irradiance. Additionally, the average over all samples for each case is shown.

Device	0 V (sun)	V_{mpp} (sun)	Total *V*-range (sun)
DCV5T-Me	0.45	0.41	0.36
Cascade	0.49	0.42	0.39
F_4-ZnPc	0.54	0.46	0.34
BDP-OMe	0.55	0.43	0.34
Ph_2-benz-BODIPY	0.55	0.41	0.37
Average	0.52	0.43	0.36

B. *EQEjV*-characteristic

After measuring the dark current (see Fig. S30 supplementary material) and the photocurrent density of a device, both can be combined to the total *jV*-characteristic by simple current addition. The results for the DCV5T-Me solar cell are shown in Fig. 3(a) and for the cascade solar cell in Fig. 3(b). The *EQEjV* was calculated for four different ways of constructing the photocurrent density over the voltage. First, it was calculated for a construction of the photocurrent density from the *dEQE* without bias illumination (*DSR*, dark) and second from the *dEQE* with AM1.5g equivalent bias irradiance (*DSR*, 1 sun). For the third calculation, the mathematical correction to the absolute *EQE* was performed only at the bias irradiance dependent measurement series without bias voltage. The obtained relation between the *dEQE* without illumination and the calculated absolute *EQE* was applied to the *dEQE*-spectra without bias illumination at all other voltages (*SR*, 0 V). For the fourth calculation, the mathematical correction to the absolute *EQE* was performed at each voltage point individually (*SR*, AM1.5g). The obtained *EQEjV* are compared with the standard mismatch corrected *jV*-measurement (*IV*). For more details of the *jV*-measurement and the total measurement procedure, see Sec. II B and Secs. VII–IX in the supplementary material. Additionally, the solar cell performance parameters (j_{sc}, V_{oc}, *FF*, and PCE) for all investigated samples and for different ways of

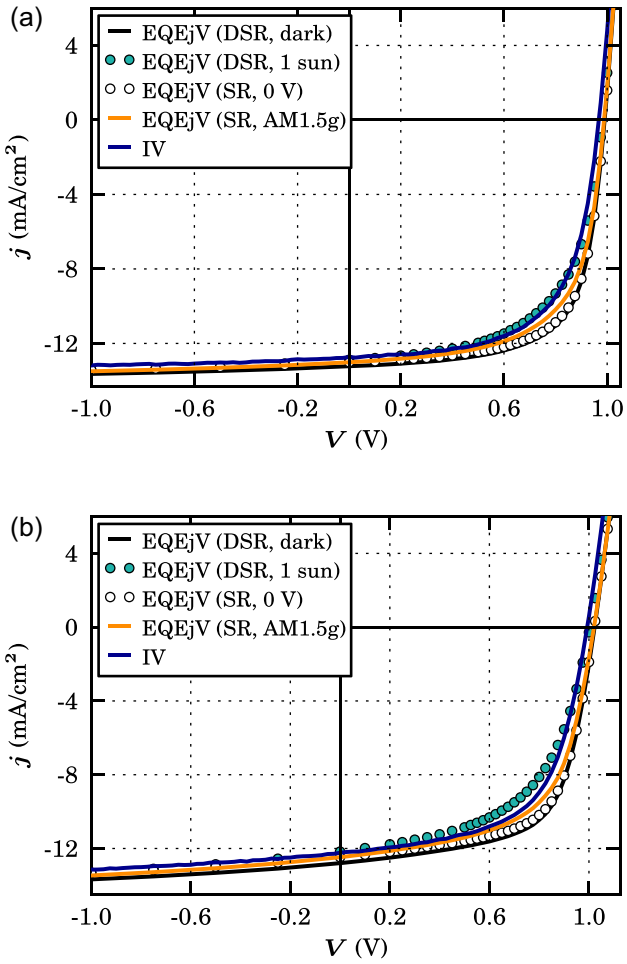

FIG. 3. Comparison of the standard, mismatch corrected *jV*-measurement (IV) with the results obtained by the *EQEjV*-method calculated from the dark-characteristic and the different constructions of the photocurrent density for (a) the DCV5T-Me device and (b) the cascade. The photocurrent density was constructed from the *dEQE* without bias illumination (*DSR*, dark) and with AM1.5g equivalent bias irradiance (*DSR*, 1 sun). Furthermore, the photocurrent density was constructed by performing the mathematical correction only at 0 V and using the obtained relation between differential and absolute *EQE* to correct the *dEQE* at all other voltages (*SR*, 0 V). Last, the photocurrent density was calculated by performing the mathematical correction at each voltage point individually (*SR*, AM1.5g).

calculating the *EQEjV* are shown in Table II. We note, that we observed a slight degradation of the DCV5T-Me and the cascade solar cell during the total measurement series. The comparison of the stability measurements before and after the total measurement series can be found in the supplementary material (see Figs. S22–S26 in Sec. VII supplementary material).

The largest deviations of the *EQEjV* compared to the standard *jV*-measurement are obtained for the construction of the photocurrent density from the *dEQE* measurements without bias illumination. For the two samples with a strong sublinear behavior of the photocurrent with irradiance (DCV5T-Me and cascade), the j_{sc} is overestimated. The *FF* is overestimated for all investigated samples caused by an overestimation of the photocurrent density over the whole voltage range. When performing the mathematical correction only at 0 V, we obtain the correct j_{sc}, but the *FF* is still overestimated. Both constructions of the photocurrent density neglect the increasing dependence of the photocurrent density with irradiance for increasing forward voltages, which was observed for all investigated samples (see Fig. 2 and Figs. S19–S21 in the supplementary material). The deviations for both constructions decrease for a weaker sublinear behavior of the photocurrent with irradiance (see Table II devices F_4-ZnPc, BDP-OMe, and Ph_2-benz-BODIPY). Thus, for a linear behavior of the photocurrent density with irradiance at all voltages, the *EQEjV* constructed from the *dEQE*-spectra without bias illumination yields an accurate *jV*-characteristic. The *EQEjV* constructed from the *dEQE* with AM1.5g equivalent illumination seems to yield the best agreement regarding the PCE when compared with the standard *jV*-measurement, especially for the samples with a weak dependence of the photocurrent on irradiance. However, for the DCV5T-Me and cascade solar cell with a stronger dependence of the photocurrent on irradiance, it is apparent that the *FF* of the *EQEjV* is clearly too low. The underestimated *FF* is caused by an underestimation of the photocurrent density, especially for higher forward voltages, when using the *dEQE* for the construction of the *EQEjV*. For higher voltages, the dependence of the photocurrent density on irradiance increases causing an increased deviation. This is clearly visible in Figs. 3(a) and 3(b) when comparing the *EQEjV*s constructed from the *dEQE* with AM1.5g equivalent bias irradiance (*DSR*, 1 sun) with the one constructed from the absolute *EQE* obtained by the mathematical correction (*SR*, AM1.5g). This, again, emphasizes the need for performing the total measurement procedure with bias irradiance dependent measurements at all voltages and performing the mathematical correction for each voltage individually. The good agreement of the *EQEjV* constructed from the *dEQE* at AM1.5g equivalent bias irradiance is caused by different measurement errors compensating each other. First of all, the already corrected j_{sc} obtained from the *EQE*-setup is generally about 1%–2.5% higher than the one yielded by the *jV*-setup pointing to inaccuracies between both setups. Furthermore, the V_{oc} obtained from the constructed *EQEjV* is generally higher than that of the *jV*-measurement. Two different aspects contribute to the error of the V_{oc}. First, the slightly higher photocurrent density of the *EQE*-setup compared to the *jV*-setup results in a small shift of the V_{oc} for the *EQEjV*. Second, there are differences between the non-illuminated and illuminated diode-characteristic of the solar cells, which is explained in the following. The photocurrent density can be obtained from the standard *jV*-measurement by subtracting the independently measured, non-illuminated diode-characteristic. For all investigated samples, the photocurrent density exceeds 0 mA/cm^2 for forward voltages above the V_{oc}, which is in contrast to the expected asymptotic behavior (see Figs. S6b–S11b in the supplementary material). Thus, the current density of the diode-characteristic is underestimated in the injection regime of the diode when using the non-illuminated diode-characteristic for the construction of the *EQEjV*. The too low current density points to a rise of the conductivity of the device under illumination. This effect was already observed by Gilot *et al.*[6] and explained with an increased conductivity due to a

rise of temperature under illumination of the device. Moreover, an increased conductivity can be caused by a filling of trap states under illumination as well as a photoconductivity effect of certain materials. This underestimated current density leads to a decreased slope of the *EQEjV* in the injection regime and, hence, to an overestimation of the V_{oc} and an underestimation of the *FF* of the device. However, in our case, the simultaneous errors of the higher V_{oc} and the higher j_{sc} compensate each other regarding the *FF*. The *FF* of the constructed *EQEjV* (*SR*, AM1.5g) and the standard *jV*-characterization are in very good agreement for all investigated samples (see Table II). The deviations of the PCE between both measurements are mainly caused by the higher V_{oc} and higher j_{sc}. Even though, the construction of the *EQEjV* was still performed with the non-illuminated diode-characteristic due to its easy accessibility in contrast to the illuminated diode-characteristic. Accounting for the mentioned errors, the most accurate reconstruction of the *jV*-characteristic for the investigated samples is obtained for construction of the photocurrent density from the total measurement series with varying applied bias voltage and a varying bias irradiance at each voltage. Additionally, the mathematical correction to the absolute *EQE* has to be performed at each voltage point individually to account for the altered dependence of the photocurrent density with respect to bias irradiance at different voltages (see Table II).

TABLE II. Comparison of the solar cell performance parameters obtained with the standard mismatch corrected *jV*-characterization (*IV*) with the results obtained by the *EQEjV*-method calculated with different constructions of the photocurrent density for all investigated samples. The photocurrent density was constructed from the *dEQE* without bias illumination (*DSR*, dark) and with AM1.5g equivalent bias irradiance (*DSR*, 1 sun). Furthermore, the photocurrent density was constructed by performing the mathematical correction only at 0 V and using the obtained relation between differential and absolute *EQE* to correct the *dEQE* at all other voltages (*SR*, 0 V). Last, the photocurrent density was calculated by performing the mathematical correction at each voltage point individually (*SR*, AM1.5g).

	EQEjV	j_{sc} (mA/cm^2)	V_{oc} (V)	*FF*	PCE (%)
DCV5T-Me					
IV		12.7	0.97	0.63	7.8
EQEjV	*SR* (AM1.5g)	13.0	0.99	0.63	8.1
	DSR (AM1.5g)	12.9	0.98	0.60	7.6
	SR (0 V)	13.0	0.99	0.67	8.6
	DSR (dark)	13.2	0.99	0.67	8.8
Cascade					
IV		12.2	0.99	0.60	7.2
EQEjV	*SR* (AM1.5g)	12.5	1.02	0.60	7.7
	DSR (AM1.5g)	12.2	1.01	0.55	6.8
	SR (0 V)	12.5	1.02	0.64	8.2
	DSR (dark)	12.8	1.02	0.64	8.4
F_4-ZnPc					
IV		11.8	0.73	0.65	5.6
EQEjV	*SR* (AM1.5g)	12.0	0.74	0.66	5.9
	DSR (AM1.5g)	12.0	0.73	0.64	5.6
	SR (0 V)	12.0	0.74	0.68	6.0
	DSR (dark)	12.0	0.74	0.68	6.0
BDP-OMe					
IV		13.2	0.73	0.65	6.3
EQEjV	*SR* (AM1.5g)	13.4	0.75	0.65	6.5
	DSR (AM1.5g)	13.3	0.74	0.63	6.2
	SR (0 V)	13.4	0.75	0.67	6.7
	DSR (dark)	13.4	0.75	0.67	6.7
Ph_2-benz-BODIPY					
IV		10.8	0.80	0.61	5.3
EQEjV	*SR* (AM1.5g)	10.9	0.83	0.61	5.5
	DSR (AM1.5g)	10.8	0.82	0.60	5.3
	SR (0 V)	10.9	0.83	0.63	5.7
	DSR (dark)	10.9	0.83	0.63	5.7

IV. CONCLUSION

We show that the *EQEjV*-method is a valid technique for characterization of organic solar cells by comparing it to a standard *jV*-measurement. We performed the calculation of the *EQEjV* for different constructions of the photocurrent density. We show that constructing the photocurrent density from the *dEQE* without bias illumination leads to its overestimation, whereas a construction from the *dEQE* with a bias irradiance of AM1.5g equivalent sun leads to its underestimation. Furthermore, performing the mathematical correction of the differential to the absolute *EQE* at 0 V only, leads to an overestimation of the constructed photocurrent density. In all three cases, the varying dependence of the photocurrent density with bias irradiance at different voltages is neglected. We find that the most accurate result is obtained for the measurement series with varying applied bias voltage and varying bias irradiance at each voltage. Subsequently correcting the differential to the absolute *EQE* at each voltage point individually leads to the least deviations between the *EQEjV* and the standard *jV*-characteristic. However, we show that differences in the non-illuminated and illuminated diode-characteristic lead to deviations between the *EQEjV* and the standard *jV*-measurement. For a further improvement of the accuracy of the method, a determination of the illuminated diode-characteristic with its subsequent use for the construction of the *EQEjV* is suggested. Furthermore, we find that for approximating the absolute *EQE* with the *dEQE* without bias voltage, a bias irradiance of 0.52 AM1.5g equivalent sun leads to a good estimate for the investigated evaporated small molecule organic solar cells. For approximating the photocurrent density over voltage for a total bias voltage series of the *dEQE* with respect to the AM1.5g spectrum a bias irradiance of 0.36 AM1.5g equivalent sun leads to a good estimate. This approximation can be used as fallback provision in case the total measurement procedure is not feasible or the solar cells are prone to degradation, especially in the case of sTSC. Although here we investigate only single-junctions, the conclusions can easily be transferred to measurements of subcells of multi-junction devices.

SUPPLEMENTARY MATERIAL

See supplementary material for additional data of the total characterization of the solar cells.

ACKNOWLEDGMENTS

The work was supported by the German Federal Ministry of Education and Research (BMBF) in the framework of the Projects No. 03EK3503A (Project "MEDOS") and No.

13N13720 (Project "UNVEIL"). We thank Tian-yi Li and Vasileios Christos Nikolis for providing the samples, and Tobias Günther and Andreas Wendel for processing the samples. The authors acknowledge Novaled AG, Dresden, Germany, for providing the dopants.

[1]D. Kearns and M. Calvin, J. Chem. Phys. **29**, 950 (1958).
[2]C. W. Tang, Appl. Phys. Lett. **48**, 183 (1986).
[3]Z. Xiao, X. Jia, and L. Ding, Sci. Bull. **62**, 1562 (2017).
[4]Y. Cui, H. Yao, B. Gao, Y. Qin, S. Zhang, B. Yang, C. He, B. Xu, and J. Hou, J. Am. Chem. Soc. **139**, 7302 (2017).
[5]J. Gilot, M. M. Wienk, and R. A. Janssen, Adv. Funct. Mater. **20**, 3904 (2010).
[6]J. Gilot, M. M. Wienk, and R. A. Janssen, Org. Electron. **12**, 660 (2011).
[7]R. Timmreck, T. Meyer, J. Gilot, H. Seifert, T. Mueller, A. Furlan, M. M. Wienk, D. Wynands, J. Hohl-Ebinger, W. Warta, R. A. Janssen, M. Riede, and K. Leo, Nat. Photonics **9**, 478 (2015).
[8]J. Metzdorf, Appl. Opt. **26**, 1701 (1987).
[9]C. G. Shuttle, B. O'Regan, A. M. Ballantyne, J. Nelson, D. D. C. Bradley, and J. R. Durrant, Phys. Rev. B - Condens. Matter Mater. Phys. **78**, 1 (2008).
[10]K. Cnops, B. P. Rand, D. Cheyns, B. Verreet, M. A. Empl, and P. Heremans, Nat. Commun. **5**, 3406 (2014).
[11]R. Meerheim, C. Körner, and K. Leo, Appl. Phys. Lett. **105**, 063306 (2014).
[12]J. Meiss, A. Merten, M. Hein, C. Schuenemann, S. Schäfer, M. Tietze, C. Uhrich, M. Pfeiffer, K. Leo, and M. Riede, Adv. Funct. Mater. **22**, 405 (2012).
[13]T.-Y. Li, T. Meyer, Z. Ma, J. Benduhn, C. Körner, O. Zeika, K. Vandewal, and K. Leo, J. Am. Chem. Soc. **139**, 13636 (2017).
[14]R. Gresser, M. Hummert, H. Hartmann, K. Leo, and M. Riede, Chem. - Eur. J. **17**, 2939 (2011).
[15]S. Kraner, J. Widmer, J. Benduhn, E. Hieckmann, T. Jägeler-Hoheisel, S. Ullbrich, D. Schütze, K. Sebastian Radke, G. Cuniberti, F. Ortmann, M. Lorenz-Rothe, R. Meerheim, D. Spoltore, K. Vandewal, C. Koerner, and K. Leo, Phys. Status Solidi A **212**, 2747 (2015).
[16]T. McMahon and K. Sadlon, Sol. Cells **13**, 99 (1984).
[17]S. R. Cowan, J. Wang, J. Yi, Y. J. Lee, D. C. Olson, and J. W. P. Hsu, J. Appl. Phys. **113**, 154504 (2013).
[18]M. Mundus, B. Venkataramanachar, R. Gehlhaar, M. Kohlstädt, B. Niesen, W. Qiu, J. P. Herterich, F. Sahli, M. Bräuninger, J. Werner, J. Hohl-Ebinger, G. Uytterhoeven, U. Würfel, C. Ballif, M. C. Schubert, W. Warta, and S. W. Glunz, Sol. Energy Mater. Sol. Cells **172**, 66 (2017).
[19]D. Ray, M. Furno, E. Siebert-Henze, K. Leo, and M. Riede, Phys. Rev. B - Condens. Matter Mater. Phys. **84**, 075214 (2011).
[20]C. Deibel, Phys. Status Solidi A **206**, 2731 (2009).
[21]L. Onsager, Phys. Rev. **54**, 554 (1938).
[22]C. L. Braun, J. Chem. Phys. **80**, 4157 (1984).
[23]C. Deibel, T. Strobe, and V. Dyakonov, Adv. Mater. **22**, 4097 (2010).
[24]T. M. Clarke and J. R. Durrant, Chem. Rev. **110**, 6736 (2010).
[25]Standard IEC 60904-8:2014-05, Photovoltaic devices - Part 8: Measurement of spectral responsivity of a photovoltaic (PV) device, 2014.